ISERME 2024 Proceedings
2nd September 2024 – Sapporo, Japan
https://doi.org/10.31705/ISERME.2024.2

Effect of Fracture Stiffness in a Fault Damage Zone on Seismic Source Parameters of Induced Fault-Slip

*Gang[1] M, Sainoki[2] A and Kodama[1] J
[1]*Faculty of Engineering, Hokkaido University, Soppaoro, Japan*
[2]*Faculty of Advanced Science and Technology, Kumamoto University, Kumamoto, Japan*
*Corresponding author – Email: gangmingwei_gmw@163.com

Abstract

It is well recognized that inherent stress concentration within a fault damage zone may lead to induced fault-slip, resulting in severe damage to underground facilities. Previous research suggests that the intensity of fault-slip is influenced not only by the mechanical properties of the fault core but also by the stiffness of the surrounding rock mass, implying that fracture stiffness could be an important factor that needs to be studied. Therefore, in this study, the effect of the fracture stiffness on seismic source parameters of induced fault-slip is investigated using a mine-wide scale heterogeneous continuum model. The model is constructed based on a discrete fracture network within a fault damage zone, utilizing the crack tensor theory and boundary traction method. The fault core is simulated as a discontinuous plane with interface elements at the center of the model, and fault-slip is induced by gradually reducing the effective normal stress on the fault plane. Seismic source parameters are computed and analyzed under various fracture stiffness conditions. Seismically radiated energy is defined as the work done by the stress perturbation across a closed surface at a distance from the earthquake source, while seismic moment is calculated using the moment tensor of a seismic source in an anisotropic medium. This study investigates increasing fracture stiffness while maintaining a normal-to-shear stiffness ratio of three. Dynamic analysis results reveal a notable impact of fracture stiffness on seismically radiated energy and seismic moment, both of which decrease significantly with increasing fracture stiffness. These findings imply the importance of considering fracture stiffness for more accurate estimation of seismically radiated energy and seismic moment.

Keywords: Fault-slip; Fracture stiffness; Seismic source parameters; Heterogeneous continuum model

1. Introduction

It is well recognized that inherent stress concentration within a fault damage zone may lead to unexpected fault-slip with a large magnitude, resulting in severe damage to underground openings. Previous studies indicate that the intensity of induced fault-slip is affected by not only the mechanical properties of the fault core but also the stiffness of the surrounding rock mass, implying that fracture stiffness in a fault damage zone could be an important factor that needs to be studied. For underground mines, induced fault-slip can be a cause of rock bursts and could inflict devastating damage on underground facilities. To elucidate the mechanism of induced fault-slip and examine its relationship with mining activity, seismic monitoring has been performed in a number of deep underground mines [1]. Furthermore, field observations of induced fault-slip indicate the variation in the spatial distribution and source parameters of induced fault-slip prior to the occurrence of intense seismic events [2]. Specifically, this includes the increases in seismically released energy and seismic moment. Therefore, many studies suggest the use of seismic source parameters as precursory information for seismic events.

Although the effects of fracture network on the occurrence of induced seismicity have been clarified, such studies were performed by incorporating a fracture network into a cube-shaped model with an edge length of 5m constructed in the framework of the discrete element method. The method cannot be directly applied to a mine-wide scale numerical model. To overcome this limitation, Sainoki et al. [3] developed a method to reproduce the complex and heterogeneous stress state on a mine-wide scale by constructing an equivalent continuum model considering the elasticity of macro fractures, based on the crack tensor theory developed by Oda [4].

Considering the discussion above, this study aims to simulate a complex stress distribution on a fault damage zone using a heterogeneous mine-wide scale model. Then, the effect of fracture stiffness on the source parameters such as seismically released energy and seismic moment is analyzed.

2. Materials and Methods

2.1 Model construction

A model with a dimension of 100m×100m×100m is constructed and the fault core is simulated as a discontinuous plane with interface elements at the center of the model (Figure 1). To generate a fracture network in a fault damage zone, the following parameters need to be determined: fracture density, fracture length, and fracture orientation. The following power law function is employed.

$$P = \alpha d^{\beta} \tag{1}$$

where, α represents a coefficient related to the maximum fracture density near a fault core; β is a scaling factor; and d is the distance from the fault core. Regarding fracture length, the following cumulative density function is employed.

$$F = \frac{l_{min}^{1-a} - l^{1-a}}{l_{min}^{1-a} - l_{max}^{1-a}} \tag{2}$$

where, a is a scaling exponent dictating the ratio between smaller and larger fractures; l_{max} and l_{min} denote the maximum and minimum fracture length simulated, respectively. Lastly, as for fracture orientation, the Fisher function expressed with the following equation is used.

$$f(\theta) = \frac{k \sin\theta exp(k\cos\theta)}{exp(k) - exp(-k)} \tag{3}$$

where, θ denotes the angular deviation from the mean vector; κ is a dispersion factor that determines the degree of the angular deviation. Using this formula, disk-shaped fractures in a fault damage zone are statistically generated (Figure 2). The present study uses the following parameters for Eqs. (1) to (3): α=30, β=0.8, lmax=10 m, lmin=2 m, a=2.5, and, κ=40. Information of these fractures located in the fault damage zone is extracted by locating fractures in a corresponding area, thus giving a list of characteristics of fractures contained in each zone of the model.

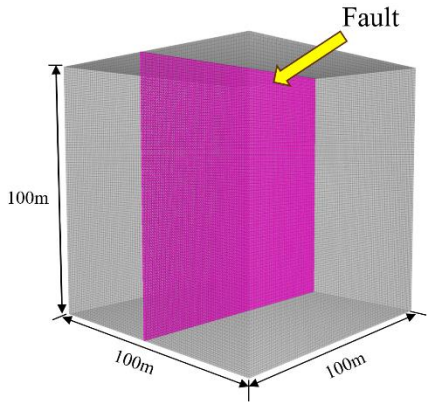

Figure 1 3D Numerical model

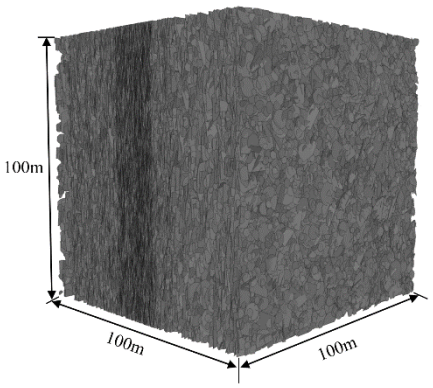

Figure 2 Fracture network

After obtaining the information, an equivalent continuum method is employed. The crack tensor theory is applied in this study to calculate an equivalent elastic compliance tensor because of its simplicity and a small number of input parameters. The equivalent compliance tensor is calculated as below.

$$F_{ij} = \frac{1}{V}\frac{\pi}{4}D^3 n_i n_j \tag{4}$$

$$F_{ijkl} = \frac{1}{V}\frac{\pi}{4}D^3 n_i n_j n_k n_l \tag{5}$$

$$C_{ijkl} = \sum_1^{NCR}\left[\frac{1}{K_n D} - \frac{1}{K_s D}\right]F_{ijkl} + \frac{1}{4K_s D}\left(\delta_{ik}F_{jl} + \delta_{jk}F_{il} + \delta_{il}F_{jk} + \delta_{jl}F_{ik}\right) \tag{6}$$

$$T_{ijkl} = C_{ijkl} + M_{ijkl} \tag{7}$$

where *F* and *n* are the crack tensor and the unit normal vector of the fracture, respectively. *C*, *M* and *T* represent the anisotropic compliance tensor equivalent to the elasticity of the fractures, the isotropic compliance tensor of the rock mass and the anisotropic compliance tensor of fault damage zone, respectively. *NCR* is the total number of fractures; *K*n and *K*s are normal and shear stiffness of the fracture, respectively; δ is the Kronecker's delta and *D* donates the diameter of the fracture. Eventually, the equivalent compliance tensor *T* considering all the effect of macro, meso, and micro fractures on the elastic matrix of the rock mass is input to a zone in the continuum model.

2.1 Simulation of seismic events

As the first step, an initial stress state is simulated by applying regional stresses to the model external boundaries. It is to be noted that the direction of gravity is rotated at 20° in anticlockwise direction to simulate a fault dipping at 70°. The reason why such a vertical fault is simulated in Figure 1 is that a complicated procedure needs to be taken to generate a DFN for dipping faults. As shown in Figure 3, the magnitude stress applied to the left boundary differs from that of the right boundary because of the rotated regional stress. The stress applied to the model boundary corresponds to those at a depth of 2000 m. As for the bottom boundary, the displacement in all directions is fixed at the four vertices to prevent the rigid body

movement. Except for the four vertices, the displacement on the bottom boundary is constrained only in the z-direction.

After simulating the initial stress state, the effective normal stress on the fault plane is gradually decreased in a stepwise manner in the circular region on the fault as shown in Figure 4. The radius of this circular region is 25 m. In each analysis stage, the effective normal stress is decreased by 0.5 MPa. Cumulatively, 20 MPa of the effective normal stress is decreased. This method assumes that on-fault induced seismicity is caused by unclamping of faults, i.e., the effective normal stress reduction due to rock mass excavation, fluid injection.

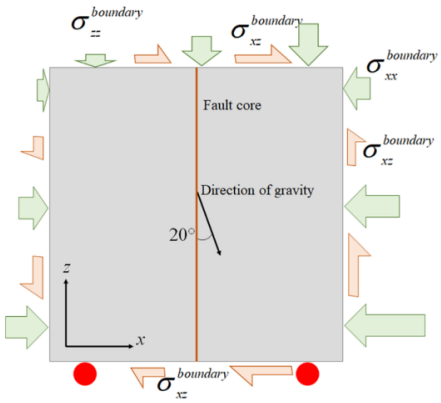

Figure 3 Boundary conditions

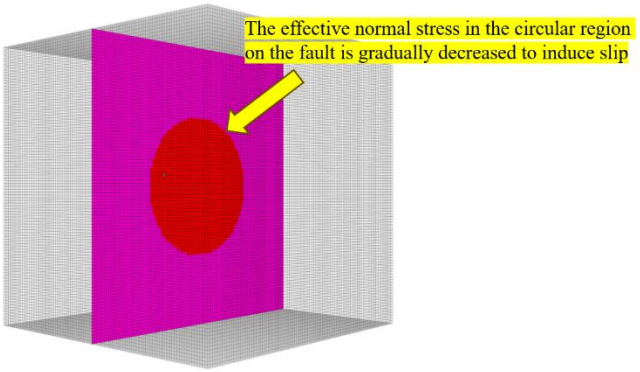

Figure 4 Effective normal stress reduction

3. Results and Discussion

In this study, seismic moment is calculated by the moment tensor of a seismic source in an anisotropic medium [5], whereas seismically radiated energy is defined as the work done by the stress perturbation across a closed surface located at a distance from the earthquake source [6]. Figure 5 shows the seismic moment for each analysis stage, highlighting the differences among the analysis stage. As shown, the seismic moment starts to increase in 8th stage. Then it takes the maximum value in 20th stage. Thereafter, the seismic moment starts to decrease. Under the condition where Kn is 30 GPa/m and Ks is 10 GPa/m, the maximum value of seismic moment is approximately 2.75×10^{9} Nm. However, under the condition where Kn is 90 GPa/m and Ks is 30 GPa/m, the maximum value of seismic moment is approximately 7.5×10^{8} N·m. The seismic moment decreases significantly with the increasing fracture stiffness with a reduction of about 72 %.

Figure 6 illustrates the seismically released energy for each analysis stage. As can be seen, the seismically released energy starts to increase in 22th stage. Then it takes the maximum value in 29th stage. Thereafter, the seismically released energy starts to decrease. Under the condition where Kn is 30 GPa/m and Ks is 10 GPa/m, the maximum value of seismically released energy is approximately 1.0×10^{5} J. However, under the condition where Kn is 90 GPa/m and Ks is 30 GPa/m, the maximum value of seismically released energy is about 3.6×10^{4} J. The seismically released energy also decreases markedly with the increasing fracture stiffness, the reduction is about 64 %.

The present study applies the crack tensor theory to construct an equivalent continuum model discretized into millions of zones in the framework of the finite difference method, where each zone has a different anisotropic compliance matrix corresponding to the characteristic of a local fracture network in a fault damage zone. A fault plane is simulated with interface elements at the center of the model. Using the model, a complex, heterogeneous stress state with stress anomalies is simulated by applying stresses on the model outer boundaries.

Seismicity is induced by decreasing the effective normal stress on the fault plane by 0.5 MPa in each analysis stage. The results indicate that both the seismically radiated energy and seismic moment decrease with the increasing fracture stiffness and imply that considering fracture stiffness is important in estimating the seismic parameters.

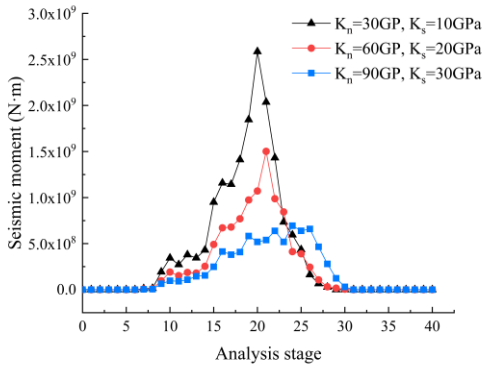

Figure 5 Seismic moment change

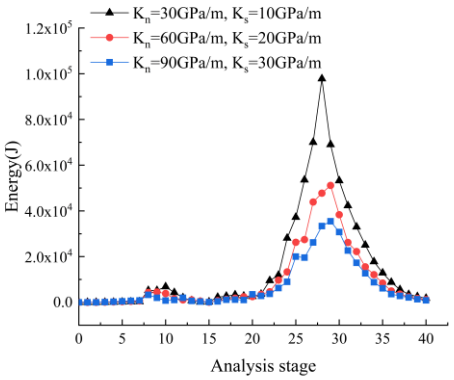

Figure 6 Seismically released energy change

References

[1] X. MA, et al. Imaging of temporal stress redistribution due to triggered seismicity at a deep nickel mine. Geomech Energy Environ 5: 55–64. 2016. doi.org/10.1016/j.gete.2016.01.001

[2] Zhang, Penghai, et al. Microseismicity induced by fault activation during the fracture process of a crown pillar. Rock Mechanics and Rock Engineering, 2015, 48: 1673-1682.

[3] A. Sainoki, et al. Numerical modeling of complex stress state in a fault damage zone and its implication on near-fault seismic activity, 2021. JGR Solid Earth. https://doi.org/10.1029/2021JB021784

[4] M. Oda, et al. An equivalent continuum model for coupled stress and fluid flow analysis in jointed rock masses. Water Resour Res ,1986, 22:1845-1856.

[5] Vavryčuk, Václav. Focal mechanisms in anisotropic media. Geophysical Journal International, 2005, 161.2: 334-346. https://doi.org/10.1111/j.1365-246X.2005.02585

[6] Rivera, Luis. Representations of the radiated energy in earthquakes. Geophysical Journal International, 2005, 162.1: 148-155. https://doi.org/10.1111/j.1365-246X.2005.02648.x